Centre for Geo-Information

Thesis Report GIRS-2004-09

MULTITEMPORAL LANDSAT IMAGES FOR VEGETATION CLASSIFICATION IN THE FLOODPLAINS (THE NETHERLANDS)

Monika Bajimaya

FEBRUARY 2004

WAGENINGEN UNIVERSITY
WAGENINGEN UR

Centre for Geo-Information

Thesis Report GIRS-2004-09

MULTITEMPORAL LANDSAT IMAGES FOR VEGETATION CLASSIFICATION IN THE FLOODPLAINS (THE NETHERLANDS)

Monika Bajimaya

FEBRUARY 2004

WAGENINGEN UNIVERSITY
WAGENINGEN UR

MULTITEMPORAL LANDSAT IMAGES FOR VEGETATION CLASSIFICATION IN THE FLOODPLAINS (The Netherlands)

Submitted By
Monika Bajimaya

Thesis submitted in partial fulfillment of the degree of Master of Science in Geo-information Science at Wageningen University and Research Center

Supervisors
Dr. Ir. Jan Clevers
Drs. Gertjan Geerling

Examiners
Dr. Ir. Jan Clevers
Drs. Gertjan Geerling
Dr. Gerrit Epema

February 2004

WAGENINGEN UNIVERSITY
WAGENINGEN UR

Acknowledgement

First of all I would like to express my sincere gratitude to my first supervisor Drs. Gertjan Geerling who gave me continuous guidance and encouragement while undertaking the thesis. I would like to thank him for introducing me to the study area. Above all, I really appreciate his availability, coming all the way from Nijmegen to Wageningen whenever needed.

I am deeply indebted to my second supervisor Dr. Ir. Jan Clevers for his invaluable help and advice, without whose guidance this thesis wouldn't have been completed. His continuous guidance while writing the report was of great help.

I would like to express my sincere gratitude to Dr. Gerrit Epema as being my examiner. I would also like to thank Willy Ten Haaf for his help and guidance throughout the study period. I would like to thank Drs. Harm Bartholomeus for his technical help.

I am grateful to all the MGI friends in Alterra. It was a great privilege to come to Wageningen and know friends from all over the world. I will never forget those beautiful years I spent in Wageningen.

Last but not least, I would like to thank my family who have always been very supportive and a good source of inspiration for me.

Abstract

Over the past few decades, satellite data have become one of the primary sources for obtaining information about the various vegetation types on the earth. In addition, multitemporal imagery is needed to monitor various vegetation types characterized by high temporal variability.

In this study, Landsat Thematic Mapper images of July, September and the combined images are used for the classification of vegetation along the floodplains of the river Waal. Different classification methods have been used to check the classification accuracy of single and combined images. A new approach, CART (Classification and Regression Tree) classification, which is a decision tree classifier is compared with the conventional methods like Maximum likelihood and the Minimum distance. Comparative study is also being done for single and combined images.

Maximum likelihood performed better than other classifiers. The overall classification accuracy obtained was higher for Maximum likelihood classification than for others.

The combined image also gave better results than the single image mainly with the MD classifier. The overall classification accuracy obtained by all the three classifiers was quite satisfactory.

Keywords: CART, Classification, Decision tree, Floodplains, Remote Sensing, Landsat TM imagery, Multitemporal, Vegetation types,

Abbreviations

CART	Classification and Regression Tree
DTC	Decision Tree Classification
GCPs	Ground Control Points
IFOV	Instantaneous Field of View
MIR	Middle Infrared
NIR	Near Infrared
MLHD	Maximum Likelihood Classification
MDC	Minimum Distance Classification
MSS	Multispectral Scanner
RMS	Root Mean Square
TIR	Thermal Infrared
TM	Thematic Mapper
UDT	Univariate Decision Tree

Table of Contents

List of Figures

List of Tables

1 Introduction

1.1 Background

The River Rhine is one of the major waterways of the European continent. It rises in the Alps, flows north and west for 1,320 kilometers with a floodplain area of 185,000 sq.km. On its way it passes through Switzerland, Germany, France and the Netherlands and finally discharges into the North sea. In the Netherlands the river is in its lower course and it flows into many distributaries of which the major one is the River Waal.

The Netherlands is a country where 75% of the land is below sea level. In the last decades of the 20th century, there have been problems with high water discharges along the river Rhine several times; especially the flooding problems in the winter of 1993/1994 and 1994/1995 need to be mentioned. The Dutch have defended themselves against the sea for centuries by an elaborate network of dikes. The high water discharges in the winter of 1994/1995 constituted a turning point in the history of water and river management in the Rhine basin. A general assembly of the river Rhine riparian states decided that further constriction of the floodplains of the river Rhine had to be counteracted and that the river needed to regain its hydrological resilience. This resulted in a Flood Action Plan to develop a new approach for river basin management (IKSR, 1997).

In the Netherlands, the flooding problems of the nineties have considerably influenced the way in which river managers deal with flooding risks. The decades-old plans for dike reinforcements were reviewed, revised and carried out. However, since the land is slowly subsiding and climate change causes sea level rise and increases the peak discharges of the rivers, it is clear that however high the dikes are, they can only provide protection against flooding to a certain level. Current strategies for flood prevention attempt to prevent dike reinforcements, because these measures are very expensive and would result in a considerable loss of natural values and cultural heritage.

So, the new water management policy emphasized the need of a sustainable water management strategy creating more space for the river, reducing the flooding risks. There are possibilities of creating room for rivers by floodplain lowering and reconstructing secondary channels but this will alter the ecological processes, removing the existing vegetation. Special attention must be paid to the vegetation succession since vegetation plays a very important role in the discharge capacity of the river. For example, floodplain forests increase the hydraulic roughness, causing more risks of floods in the land behind the dikes.

Due to the increase in the vegetation dynamics, and its impact on the discharge capacity of the rivers, more frequent and accurate ways of monitoring vegetation changes in the floodplains need to be developed, enabling the river manager to act quickly and effectively against flooding. Monitoring results provide the river manager with information on the present state of the floodplains and will in time make an analysis of important processes possible (Van der Lee *et al*., 2001).

Regarding the monitoring of vegetation, different remote sensing techniques can be applied for classification of vegetation types, which may be a valuable tool for river management.

1.2 Problem Definition

Landsat Images are useful to track changes in large river basins. Maps resulting of Landsat classification could be used as input in 1-dimensional hydraulic models to calculate the large-scale effects of discharge peaks in the river and its floodplains. Preliminary classification of a single Landsat image gave promising results, but some classes could not be distinguished (Van der Lee *et al*., 2001, Geerling *et al*., 2001). The spectral reflectance of vegetation changes during the season, and is different for each vegetation type. For a particular image different vegetation types often show a similar spectral response and are difficult to separate. So, the use of more than one satellite image is then required for proper classification of vegetation types.

1.3 Objectives

The main aim of the research is to study the merit of combining two Landsat images, thus to improve the classification of vegetation as compared to a monotemporal image, and to generate a vegetation map of the floodplains along the river Waal.

More detailed objectives are:

- To classify natural vegetation types by using multitemporal Landsat- TM images.
- To study the improvements by using a decision tree classification algorithm.
- To compare the classification accuracies yielded by decision tree algorithms and conventional classification algorithms such as Maximum likelihood classification/ Minimum Distance classification used in remote sensing.
- To compare the classification accuracies yielded by a single Landsat image with that yielded by the combined Landsat images of two different months.

1.4 Research Questions

1. Which approach gives the best classification accuracy: Maximum likelihood / Minimum Distance or Decision tree classification?
2. What is the accuracy obtained from single and combined Landsat images?
3. Is Decision Tree Classification a suitable approach for vegetation classification using Multitemporal Landsat-TM image in comparison to ML and MD classifications?

1.5 Set-up of the report

Chapter 1: gives introduction to the main theme, the objectives, problem definition and the research questions of the thesis.

Chapter 2: deals with the literature review part, basically describes the concept of decision tree classification.

Chapter 3: covers the methodological aspect of the study

Chapter 4: reports the results obtained from the data analysis and processing and discussion of the results.

Chapter 5: contains conclusion made out of the results obtained and also gives recommendations on how the results can be improved for further studies.

2 Literature Review

2.1 Floodplain Definition

A floodplain is defined as a lowland area, dyked, floodproofed, or unprotected, which is at an elevation susceptible to flooding. Floodplain areas are relatively flat surfaces adjacent to active stream or river channels, formed by deposition of sediments during major floods.

Floodplains can be looked at from several different perspectives: 'To define a floodplain depends somewhat on the goals in mind. As a topographic category it is quite flat and lies adjacent to a stream; geomorphologically, it is a landform composed primarily of unconsolidated depositional material derived from sediments being transported by the related stream; hydrologically, it is best defined as a landform subject to periodic flooding by a parent stream. A combination of these [characteristics] perhaps comprises the essential criteria for defining the floodplain" (Schmudde, 1968). Most simply, a floodplain is defined as "a strip of relatively smooth land bordering a stream and overflowed [sic] at a time of high water"(Leopold *et al.*, 1964).

2.2 Existing methods for floodplain vegetation mapping

Generally, two methods are used for vegetation mapping in the floodplain areas in the Netherlands. One is the small-scale field mapping done by actual field sampling, walking over the borders of each class with GPS which is very precise but very time consuming at the same time and is mainly used for mapping vegetation for ecological purposes (Van der Lee *et al*., 2001, Geerling *et al*., 2001). The other is the large-scale manual photograph mapping that is the visual interpretation of the true color aerial photographs (Asselman, 2001).

2.3 Remote sensing for floodplain vegetation monitoring

Remote sensing offers the opportunity to monitor landuse/landcover conditions in a repeated and cost-efficient manner over large areas (Song and Woodcock, 2003).

During the past two decades, computer-assisted vegetation classification and monitoring using satellite images has been widely applied (Cracknell, 1999) for its effectiveness in time, labour and cost, especially for studies at regional scales. Satellite data have become one of the primary sources for obtaining information about the vegetation on the Earth's land surface. Among various remotely sensed data, Landsat imagery is frequently used for vegetation change study, because of its high resolution and good continuity in temporal series.

Vegetation classification is one of the most widely used applications of remote sensing. Since the launch of the first satellites in the early 1970s, great effort has been devoted to developing and improving the methodology to define land cover classes.

2.4 Importance of multitemporal analysis

Although single-date snapshots may be sufficient for some applications, other research relies on multi-temporal data (Pax-Lenney and Woodcock, 1997). For a particular image different vegetation types often show a similar spectral response and are difficult to separate. So, the use of more than one satellite image is then required for proper classification of vegetation types.

The optimum number of images needed can be difficult to determine. Classifications of landscapes characterised by seasonal vegetation features [e.g., deciduous forests (Kalensky and Scherk, 1975; Wolter *et al*., 1995) and agricultural fields (Steiner and Maurer, 1969; Badhwar *et al*., 1982)] show improved accuracy when derived from multidate imagery compared with single-date imagery. Wagner *et al*. (1993) found that both overall and average class accuracies for a site in Colorado improved with the use of spectral data from three dates (in a single summer season) compared with results obtained when using data from one or two dates. On the other hand, classification accuracy can be significantly improved by using multi-season imagery (Jeon and Landgrebe 1999) and multi-sensor data (Dai and Khorram 1998, Michelson *et al*., 2000, Liu *et al*., 2002).

2.5 Decision tree techniques and remote sensing

A wide variety of techniques have been used to classify vegetation over large areas from satellite data. Techniques range from unsupervised clustering algorithms (e.g., Loveland and Belward, 1997) to parametric supervised algorithms such as maximum likelihood (e.g., DeFries and Townshend, 1994; Tucker *et al*., 1985) to machine learning algorithms such as decision trees (e.g., Friedl *et al*., 1999).

Decision trees for remote sensing applications were already evaluated on satellites such as Landsat in the 1970s (Swain and Hauska 1977). Yet, only in recent years did this method gradually emerge from business applications into natural science and provided successful land cover classifications (Hansen et al. 1996, Brodley *et al*., 1999, Lawrence and Wright 2001, Vogelmann *et al*., 2001). Decision tree theory (Breiman *et al*., 1984) has previously been applied to land cover classification from satellite data (DeFries *et al*., 1998; Friedl and Brodley, 1997; Friedl *et al*., 1999; Hansen *et al*., 2000; 1996; Swain and Hauska, 1977).

Decision trees have several advantages over traditional supervised classification procedures used in remote sensing such as maximum likelihood classification. In particular, decision trees are strictly non-parametric and do not make any implicit assumptions regarding the normal distributions of the input data. These classifiers can also accept a wide variety of input data, including non-remotely sensed ancillary data, and in the form of both continuous and /or categorical variables. The general simplicity and hierarchical structure of the results from decision trees can also be valuable assets to both experienced and inexperienced users for interpretation, algorithm testing and refinement, and analysis. Finally, decision trees have been shown to provide improved accuracies over the use of other more traditional classifiers (Brown de Colstoum *et al*., 2003).

2.6 Decision Tree Algorithms

2.6.1 Overview

A Decision tree is defined as a classification procedure that recursively partitions a data set into smaller subdivisions on the basis of a set of tests defined at each branch (or node) in the tree (Figure 1). The tree is composed of a root node (formed from all of the data), a set of internal nodes (splits), and a set of terminal nodes (leaves). Each node in a decision tree has only one parent node and two or more descendant nodes. In this framework, a data set is classified by sequentially subdividing it according to the decision framework defined by the tree, and a class label is assigned to each observation according to the leaf node into which the observation falls.

More commonly, the splits defined at each internal node of a decision tree are estimated from training data by using a statistical procedure. The specific techniques used for this work are called "Learning algorithms", which have been developed within the machine-learning and pattern-recognition communities. They require high-quality training data from which relations among the features and classes present within the data are "learned". Therefore, a set of training samples representative of the population to be classified must be available to construct an accurate decision tree.

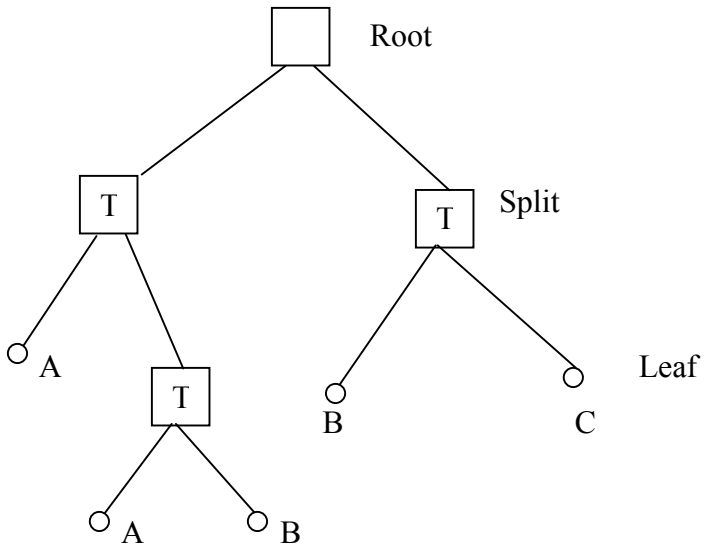

Figure 1: A decision tree classifier.
Each box is a node where tests (T) are applied to recursively split the data into successively smaller groups. The labels (A, B, C, D) at each leaf node refer to the class label assigned to each observation.

2.6.2 Univariate Decision Trees

A Univariate decision tree (UDT) is a type of decision tree in which the decision boundaries at each node of the tree are defined by a single feature of the input data (Swain and Hauska, 1969). At each internal node in a UDT, the data are split into two or more subsets on the basis of a test of a single feature of the input data. Each test is required to have a discrete number of outcomes. In this framework, a UDT classification proceeds by recursively partitioning the input data until a leaf node is reached, and the class value associated with the leaf is then assigned to the observation.

The specific values of the decision boundaries in a UDT are estimated empirically from training data. In the case of continuous data, a test of the form $X_{i.} > C$ is estimated at each internal node of a UDT from training data, where $X_{i.}$ is a feature in the data space and C is a threshold in the observed range of $X_{i.}$ The value of C is estimated by using some objective measure that maximizes the dissimilarity or minimizes the similarity of the descendant nodes, using one feature at a time. The most frequently used selection methods are the information gain, the information gain ratio [Quinlan, 1993], Gini index [Breiman *et al*., 1984]. As each test in UDT is based on a single feature, it is restricted to a split through the feature space that is orthogonal to the axis representing the selected feature.

A multivariate decision tree also exists (Brodley & Utgoff, 1995), but it is not used in this study.

A well-known example of this type of approach (UDT) is the CART model described by Breiman et al. (1984).

2.6.2.1 An Overview of the CART® Methodology

The CART analysis is a form of binary recursive partitioning. The process is binary because parent nodes are always split into exactly two child nodes and recursive because the process can be repeated by treating each child node as a parent. Thus, each parent node can give rise to two child nodes and, in turn each of these child nodes may themselves be split, forming additional children. The term "partitioning" refers to the fact that the dataset is split into sections or partitioned. CART analysis consists of four basic steps. The first step consists of tree building, during which a tree is built using recursive splitting of nodes. Each resulting node is assigned a predicted class, based on the distribution of classes in the learning dataset, which would occur in that node and the decision cost matrix. The assignment of a predicted class to each node occurs whether or not that node is subsequently split into child nodes. The second step consists of stopping the tree building process. At this point a "maximal" tree has been produced, which probably greatly over fits the information contained within the learning dataset. The third step consists of tree "pruning" which results in the creation of a sequence of simpler and simpler trees, through the cutting off of increasingly important nodes. The fourth step consists of optimal tree selection, during which the tree which fits the information in the learning dataset, but which does not over fit the information, is selected from among the sequence of pruned trees (Lewis, 2000). Each of these steps is described in detail below.

2.6.2.1.1 Splitting Rules

Tree building begins at the root node, which includes the whole learning dataset. Beginning with this node, the CART® software finds the best possible variable to split the node into two child nodes. To split a node into two child nodes, CART always asks questions that have a "Yes" or "No" answer. In order to find the best variable, the software checks all possible splitting variables (called splitters), as well as all possible values of the variable to be used to split the node (Lewis, 2000). CART® then ranks in order each splitting rule on the basis of a quality of split criterion. The default criterion

used in CART is the GINI index; essentially a measure of how well the splitting rule separates the classes contained in the parent node.

Computing Gini Index

If a data set T contains observations from n classes, gini (T) is defined as

$$\text{Gini}(T) = 1 - \sum_{j=1}^{n} P^2 j$$

Where Pj is the relative frequency of class j in T.

If a dataset T is split into two subsets T_1 and T_2 with sizes N_1 and N_2 respectively, the gini index of the split data contains observations from n classes, the gini index [gini (T)] is defined as

$$\text{Gini}_{\text{split}}(T) = \frac{N_1}{N} \text{gini}(T_1) + \frac{N_2}{N} \text{gini}(T_2)$$

2.6.2.1.2 Class Assignment

Each node has to be assigned a predicted class. This is necessary, because there is no way to know during the tree-building process which nodes will end up being terminal nodes after pruning. Once a terminal node is found, it must be decided how to classify all cases falling within it. One simple criterion is the plurality rule: the group with the greatest representation determines the class assignment. The function used to assign predicted classes to each node is defined as follows.

Criteria for assigning Classes to Nodes

C(j/i) is cost of classifying i as j.

$\pi(i)$ is prior probability of i.

N_i is number of class i in dataset.

$N_i(t)$ is number of class i in node.

Node is class i, if

$$\frac{C(j/i)\pi(i)\, N_i(t)}{C(i/j)\pi(j)\, N_j(t)} > \frac{N_i}{N_j} \quad \text{for all values of j.}$$

2.6.2.1. 3 Stopping tree building

The stopping rule for a classification tree refers to the criteria that are used for determining the right sized classification tree that is a classification tree with an appropriate number of splits and optimal predictive accuracy (Pavuluri, 2003). The tree building process goes on until it is impossible to continue. The process is stopped when there is only one observation in each of the child nodes or when all observations within each child node have the identical distribution of predictor variables, making splitting impossible.

2.6.2.1.4 Pruning Trees

Pruning is done to simplify the decision trees that overfitted the data, to generate a sequence of simpler and simpler trees. Instead of attempting to decide whether a given node is terminal or not, CART proceeds by growing trees until it is not possible to grow them any further. Once CART has generated what we call a maximal tree, it examines smaller trees obtained by pruning away branches of the maximal tree. This follows a bottom-up approach that is the pruning starts from the leaf nodes (terminal nodes) and finishes with the root node.

2.6.2.1.5 Optimal tree selection

The maximal tree will always fit the learning dataset with higher accuracy than any other tree but it overestimates the performance of the tree on an independent data set obtained from the similar dataset. The goal in selecting the optimal tree, defined with respect to the expected performance on an independent set of data is to find the correct complexity parameter $\propto$ so that information in the learning dataset is fit but not overfit. Here $\propto$ is a measure of how much additional accuracy a split must add to the entire tree to warrant the additional complexity. In general, to find the value for $\propto$ would require an independent set of data.

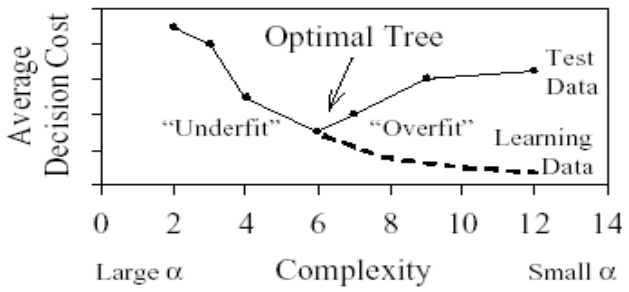

Figure 2: Relationship between tree complexity

Figure 2 shows the relationship between tree complexity, reflected by the number of terminal nodes, and the decision cost for an independent test dataset and the original learning dataset. As the number of nodes increases, the decision cost decreases for the learning dataset. This corresponds to the fact that the maximal tree will always give the best fit to the learning dataset. On contrary, the expected cost for an independent dataset reaches a minimum, and then increases as the complexity increases. As $\propto$ increases, more and more nodes are pruned away, resulting in simpler and simpler trees (Lewis, 2000)

2.6.2.1.6 Cross Validation

Another way of assessing accuracy is by V-fold cross-validation. This type of cross-validation is used if data are insufficient for a separate test sample. In such cases, CART grows a maximal tree on the entire learning sample. This is the tree that will be pruned back. CART then proceeds by dividing the learning sample into 10 roughly equal parts, each containing a similar distribution for the dependent variable. CART takes the first 9 parts of the data, constructs the largest possible tree, and uses the remaining 1/10 of the data to obtain initial estimates of the error rate of selected sub-trees. The same process is then repeated (growing the largest possible tree) on another 9/10 of the data while using a different 1/10 part as the test sample. The process continues until each part of the data has been held in reserve one time as a test sample. The results of the 10 mini-test samples are then combined to form error rates for trees of each possible size; these error rates are applied to the tree based on the entire learning sample.

3 Materials and Methodology

3.1 Study Area

The study area comprises the main part of the river Waal (Figure 3). The river Waal is the largest of the river Rhine in the Netherlands, carrying about 2/3 of the total Rhine discharge. The total surface area of the study area is about 4,250 ha.

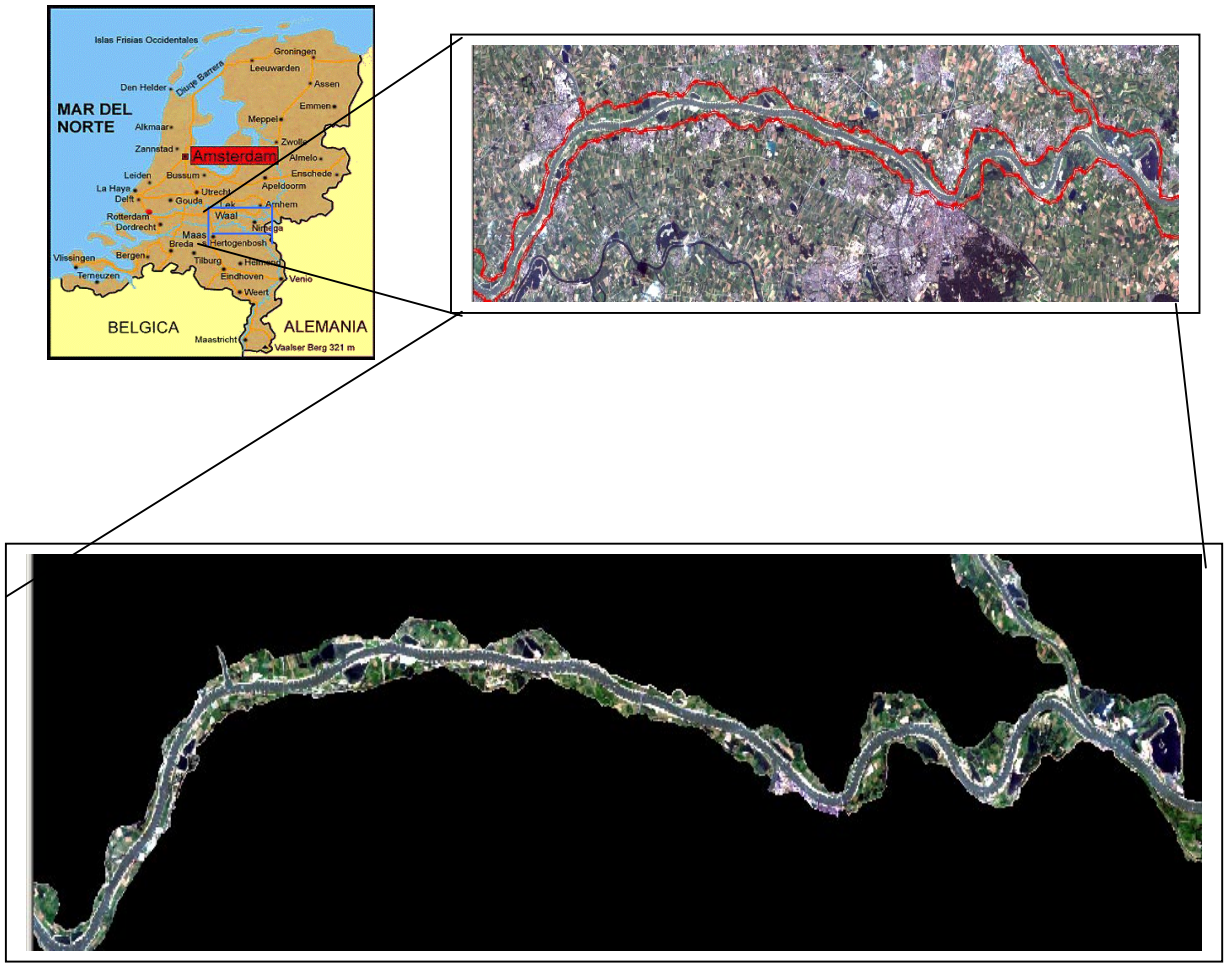

Figure 3: The Study area (The Waal)

It consists of eleven floodplains along the middle reach (circa 30 km) of the river Waal between Nijmegen and Tiel. The Waal is a Dutch branch of the river Rhine and connects the main port of Rotterdam with the German industrialised areas. Winter dikes border the floodplains and protect the hinterland against flooding.

In some floodplains, summer dikes prevent flooding of agricultural land during the growing season. The surface areas of the summer bed and floodplains are about 1,130 ha and 3,120 ha respectively. The major rivers in the Netherlands, including the river Waal, were embanked in the late middle ages to protect the low lying areas from flooding. The study area covers the embanked floodplains along the river Waal, from the bifurcation at Pannerdensche Kop to Werkendam. Nowadays, most floodplains along the river Waal are used as pasture land for cattle grazing, with local tree stands and a few fields of arable land.

3.2 Description of available Datasets

3.2.1 Aerial Photograph

Aerial photographs of the year 1999 were used as ground truth data. One aerial picture covers 2 x 2 Kilometers and its resolution is 1 m. So, all the pictures covering the study area were mosaicked using ERDAS Imagine 8.5, Mosaic Tool.

3.2.2 Ecotope map

An ecotope map of the year 1997 was also used as ground truth data. Originally, the ecotope map had 24 classes of vegetation (IVR classification), but later they were merged and the ecotope map with only 8 classes was produced. This also helped to identify the vegetation types in the study area.

3.2.3 Satellite data

Two Landsat TM images were used for this study. The images were acquired in July 1999 and September 1999. For this study, the six spectral bands (1 to 5 and 7) of the Landsat images were used, the thermal band 6 was not used.

3.2.3.1 Landsat-5™

Since 1972, Landsat satellites have provided repetitive, synoptic, global coverage of high resolution multispectral imagery. The Thematic Mapper (TM) on Landsat-5, launched in March 1984, provides information on the earth's surface in the visible, near (NIR), middle (MIR) and thermal (TIR) infrared regions of the electromagnetic spectrum.

The Thematic Mapper (TM) sensor is an advanced, multispectral scanning, Earth resources instrument designed to achieve higher image resolution, sharper spectral separation, improved geometric fidelity and greater radiometric accuracy and resolution than the Multispectral Scanner (MSS) sensor which was on board of the first Landsat satellites. The TM data are scanned simultaneously in seven spectral bands. The seven

spectral bands on Landsat have an instantaneous field of view (IFOV) of 30x30 meters in bands 1 to 5 and band 7. Band six scans thermal (heat) infrared radiation with an IFOV of 120x120 meters on the ground. With seven bands of multispectral (color) imagery, Landsat-5 TM data provides a wealth of information on ground cover and land use beyond what can be seen with the naked eye and over very large areas (Landsat 5, Sensor characteristics, 2004).

An overview of the band characteristics of the Landsat TM image is shown in Table 1.

Table 1: Spectral range of bands and spatial resolution for the TM sensor.

Landsat Bands	Wavelength (Micrometers)	Resolution (Meters)
Band 1 Blue	0.45 – 0.52	30
Band 2 Green	0.52 – 0.60	30
Band 3 Red	0.63 – 0.69	30
Band 4 Near Infrared	0.76 – 0.90	30
Band 5 Mid Infrared	1.55 – 1.75	30
Band 6 Thermal Infrared	10.40 – 12.50	120
Band 7 Mid Infrared	2.08 – 2.35	30

3.3 Methodology

The whole methodological process of this study is illustrated in Figure 3. The process is divided into four main steps:

The first step comprises:
Pre – processing of the datasets.
Preparation of training and testing sets.

The second step deals with performing the supervised classification by Maximum likelihood Classification and Minimum Distance Classification.

The third step deals with preparation of the input for the CART analysis.

The fourth step deals with the implementation of the CART analysis. Then, accuracy assessment and validation is carried out in order to make concrete conclusions on the analysis performed.

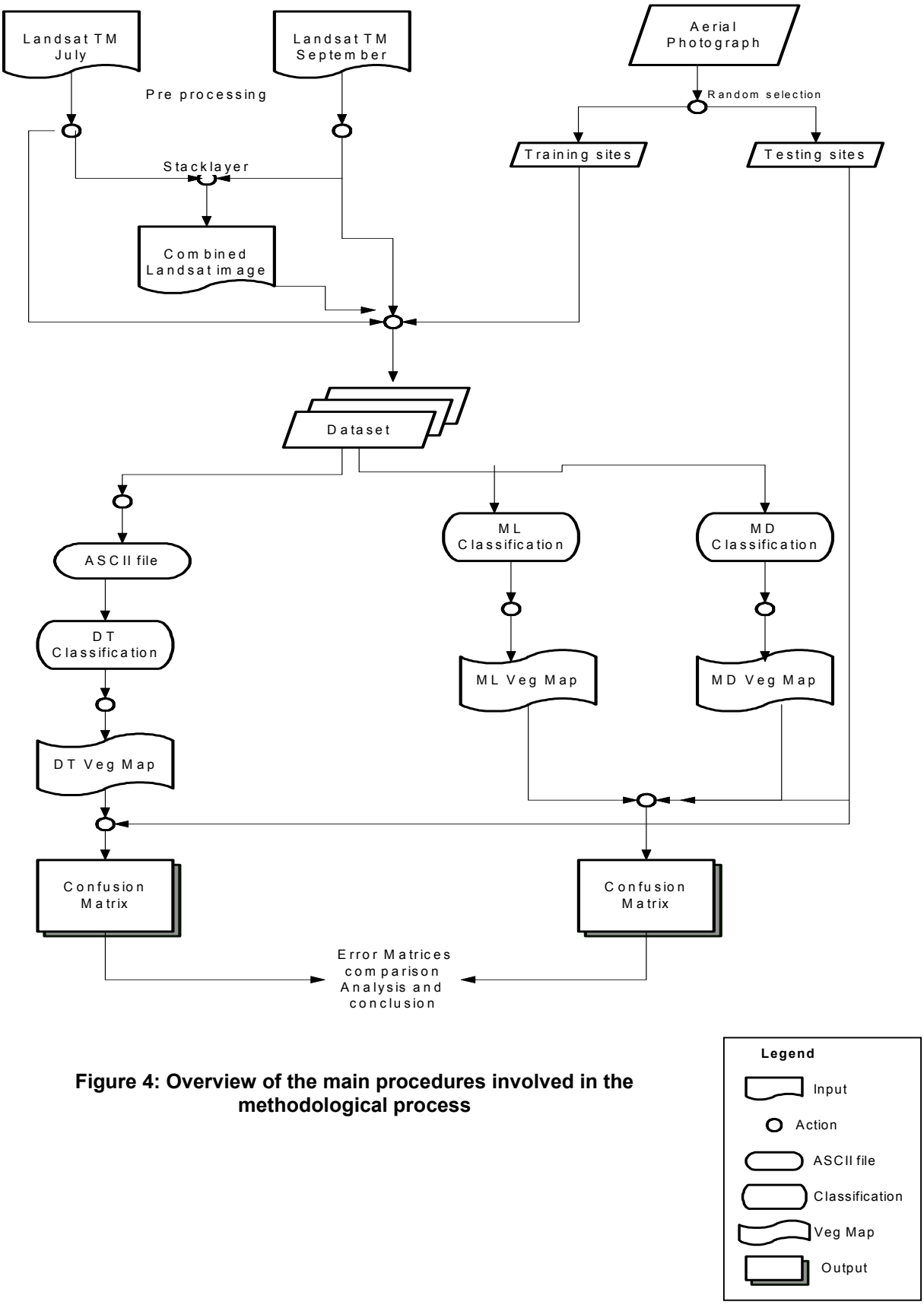

Figure 4: Overview of the main procedures involved in the methodological process

3.4 Dataset Pre- processing

3.4.1 Geometric Correction

The Landsat 5 TM images were converted to RD grid (Dutch) Coordinate System (Stereographic projection, Datum: Bessel) using a first order polynomial transformation with the nearest neighbour resampling method. First, the July image was geo-corrected using 40 ground control points, well distributed throughout the study area. The selection and extraction of the ground control points were made from the aerial photograph of the same area. The geo-correction operation was made by "Landsat Geometric Model" in ERDAS Imagine 8.5. This model takes into account the elevation (DEM) source of data in order to correct the relief displacement. However, for the flat study area, a DEM was not used, so we put the elevation source as constant. The GCP's were adjusted according to the RMS error. Then the resampling with the Nearest Neighbour procedure was done which finished the transformation process.

The September image was corrected by transforming the map coordinate system of the geocorrected July image to the September image by finding some common ground control points in both the images.

3.4.2 Training and Testing sets

Training and testing fields are areas of known identity delineated on the digital image, which are used in classification as learning paradigm for the classification of the image but also for accuracy assessment of the classification (Campbell, 1996).

The selection of the training and testing sets in the study area was done in a random way, ensuring at the same time that for each class the training and testing sets were equally spatially distributed over the whole study area. A total of 2724 training pixels were delineated on the image with reference to the aerial photograph and the ecotope map. The training dataset was used for training the classifiers and the testing dataset were used in the validation for assessing the accuracies.

For the input of the dataset into the CART, the data was converted to ASCII format. This conversion was performed using Erdas Imagine 8.5 and Microsoft Excel software.

3.5 Description of Vegetation Classes used for the study

Initially, there have been about 24 vegetation classes defined for the study area Waal, based on the ecological relevance. These 24 classes were later merged together based on their structural similarities since there is a direct relation between the structure and the hydraulic roughness of the vegetation (Asselman, 2001). Finally, 8 classes were created based on the ecological and hydrological aspects of the vegetation. The details of the different classes are described in Table 2 (Appendix II).

Table 2: Description of the vegetation classes used in this study.

Classes	Names of Classes	Description of classes
Class 1	Water	Deep Riverbed, Water formed by secondary channel, Dynamic blind river arm water, Isolated blind river arm water, Pool water, Manmade water (harbour, intensive recreation)
Class 2	Forest	Floodplain forest with Softwood and Marsh forest, Floodplain forest with hardwood
Class 3	Buildings	Manmade buildings, Bridges
Class 4	Bare soil	Shallow Riverbed, Flat river bank, Steep bank/eroding bank
Class 5	Agriculture area	Agricultural land (production forest, crop land)
Class 6	Grassland	Grassland pasture, Grassland Meadow
Class 7	Herbaceous	Herbaceous natural levee and river dunes
Class 8	Swamp	Marsh, Reed (Young Phragmites reed, Old Phragmites reed)

3.6 Merging of Landsat images (Multitemporal Analysis)

Multitemporal data merging can take place in many different ways. One such operation is simply combining images of the same area taken on more than one date to create a product useful for visual interpretation. One approach is to register all spectral bands from all dates of imaging into one master dataset for classification. For example, the six reflectance (nonthermal) bands of a TM image from one data might be combined with the same six bands for an image acquired on another date, resulting in a 12-band dataset to be used in the classification (Lillesand & Kiefer, 2000).

So, for multitemporal analysis, the two images of July and September were combined using the Stacklayer function in ERDAS Imagine 8.5. All the six reflectance bands of each image were combined, thus producing the final image with 12 bands which was used for classification.

3.6.1 Image Normalization

Factors such as atmospheric conditions, sun angle, Earth to sun distance, differences in sensors, and sun/target/sensor geometry effect the brightness values and can cause variations in brightness values from date to date. Normalization will limit the variation from date to date so that brightness values can be correlated and then related to surface conditions to correlate vegetation conditions classified in the July imagery to spectral characteristics in the September imagery.

So, after stacking the July and September images, normalization was done to correlate the brightness values in the July Landsat TM imagery with the brightness values in the September Landsat imagery. Normalization of the combined image with all the 12 bands was done by Normalize function in ERDAS Imagine 8.5.

3.7 Maximum likelihood Classification

The ML classification is the most common supervised classification method. The ML classifier was selected, as it is the most widely known and used classifier. Since one of the objectives of the study is also to compare the conventional method of classification with the decision tree, the ML classifier was chosen. ML classification uses the training data as a means of estimating means and variances of the classes (Campbell, 1996). It evaluates both the variance and covariance of the category spectral response patterns when classifying an unknown pixel. It is based on the assumption that the members of each class follow a Gaussian (normally distributed) frequency distribution in the feature space. ML is a pixel-based method, which involves the estimation of class mean vectors and covariance matrices from the training data chosen from unknown examples of each particular class. The function is used to evaluate the membership probability of an unknown pixel for a class. The pixel is assigned to the class for which it has the highest membership probability value (Lillisand & Kiefer, 2000).

3.8 Minimum-Distance-to-Means Classification

Apart from Maximum likelihood classification, Minimum Distance classification was also performed to compare classification methods.

Minimum Distance uses the central class values of the spectral data that form the training data as a means of assigning pixels to informational categories (Campbell, 1996). These values comprise the mean vector for each category. Values in several bands determine the positions of each pixel within the clusters that are formed by training data for each category. Each cluster can be represented by its centroid, often defined as its mean value. As unassigned pixels are considered for assignment to one of the several classes, the multidimensional distance to each cluster centroid is calculated and the pixel is then assigned to the closest cluster. Thus, the classification proceeds by always using the "minimum distance" from a given pixel to a cluster centroid defined by the training data as the spectral manifestation of an informational class (Lillisand & Kiefer, 2000).

3.9 Application of the CART® concept for classification

The decision tree analysis was performed by the CART® (Classification and Regression Trees) software, version 5.0 (Salford Systems, 2002). The training dataset, with unique identification number for each class (vegetation classes), and the variables layers (bands) represent the fundamental input for the CART® analysis.

All the six bands of the two images and the combined image and classes were included in the tree analysis. By this method, the CART® software can identify the most important variables and discover for each one the threshold value. The detail steps involved in CART analysis are explained in the literature review part (Chapter 2).

For this study, the 6 bands of the single image and the 12 bands of the combined image were considered the predictor variables, which are the independent variables. The unique identification number for each class represented the target variable which is a dependent variable. The class itself also represented the categorical variable, which is to be categorized according to the predictor variables. The threshold level for the categorical variables was set to 10 as we had 8 classes. The splitting method used for this study was the Gini rule, which is a default criterium used in CART. It is also one of the well-known standard splitting rule The Gini splitting rule looks for the largest class in the dataset and isolates it from all other classes. Once the first split is made, Gini continues to split the data that require further segmentation based on the same class dominant criteria.

One of the important options used in CART is Priors which helps in shaping the classification analysis. By default, the assumed priors are equal (all categories have equal probability), which means that the classes are treated as if they were uniformly distributed in the sample and each class is equally treated for classification accuracy. Similarly, for minimum node sizes, parent node minimum cases were set to 10 and terminal node minimum cases were set to 1, which are the default criteria used in CART. For testing the classification accuracy, a separate set of testing data was used instead of V-fold cross validation.

4 Results And Discussion

4.1 Signature analysis

To analyze the spectral reflectance characteristics of various vegetation types in different images spectral profiles were plotted. Figure 5, 6 and 7 show the spectral reflectance characteristics of vegetation in July, September and combined images respectively in the six bands of the Landsat TM image. Class 1 shows relatively low DN values in all the bands compared to other classes. On the contrary, class 4 shows relatively higher DN values in most bands.

These profiles of mean DN values (Figures 5, 6 and 7) show that bands 3, 4, 5 and 7 of the Landsat TM image in the visible, near infrared and middle infrared portions of the spectrum respectively show the greatest variation between the vegetation types. Therefore, they offer great potential for discrimination of various vegetation types.

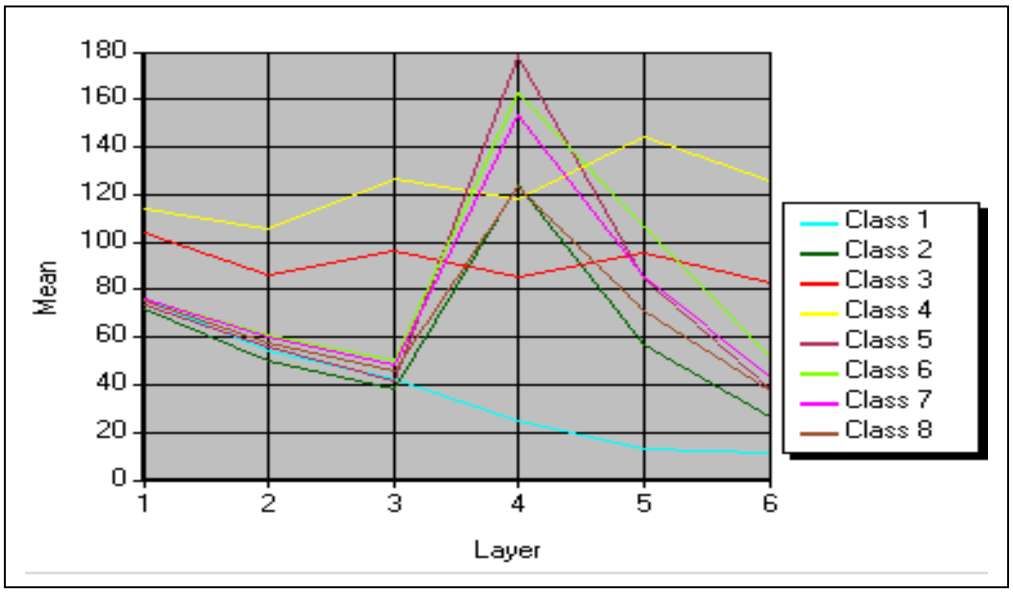

Figure 5: Spectral Profile of July image.

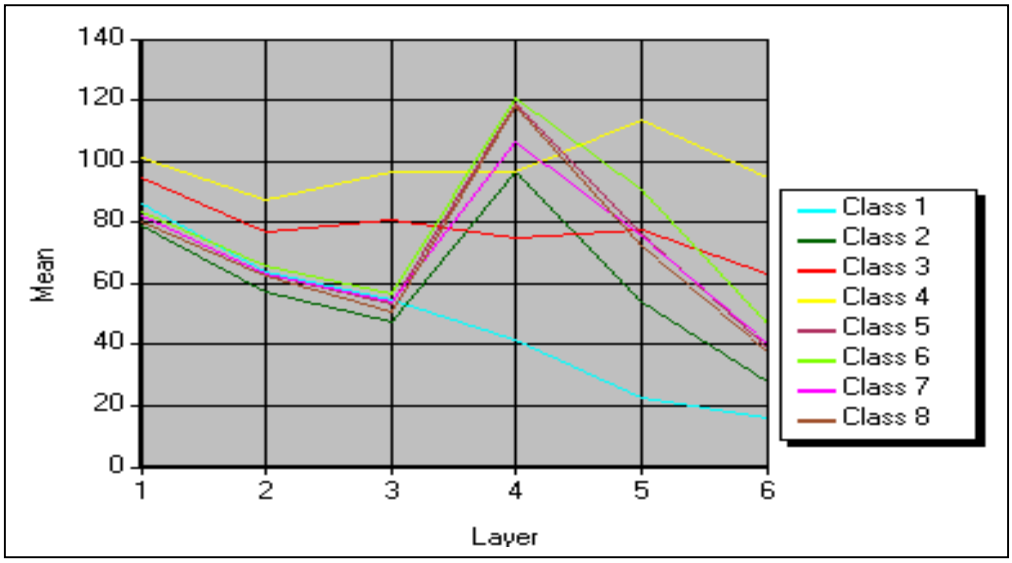

Figure 6: Spectral Profile of September image.

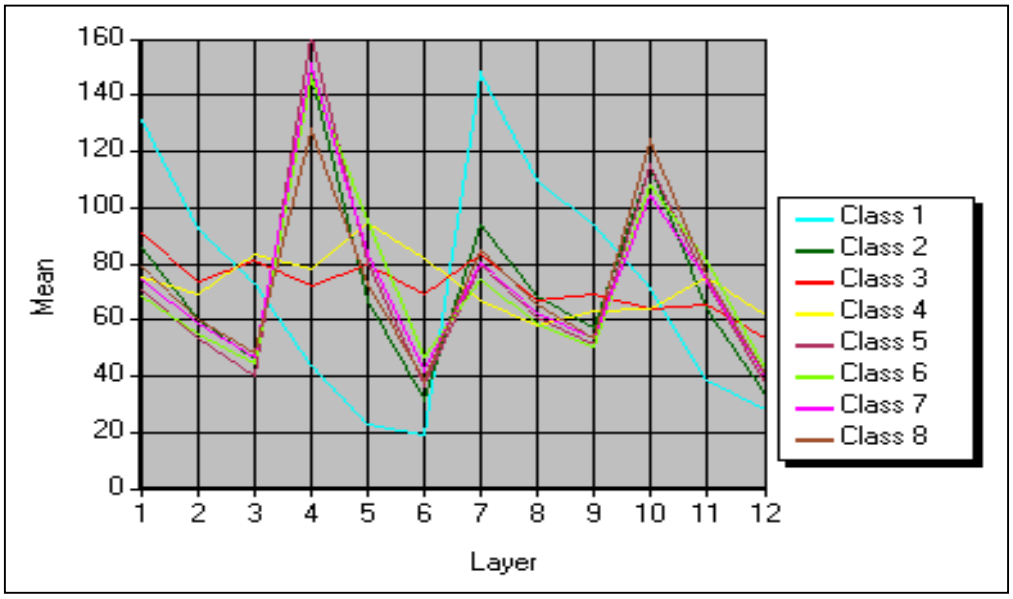

Figure 7: Spectral Profile of Combined image.

4.2 Classification Accuracy assessment

The accuracy of the classification process was evaluated using separate testing sites in the study area. For each one of the classifications the confusion matrix was generated and the overall accuracy, the producer's and user's accuracy and the Kappa statistics for each class was calculated (Lillesand & Kiefer, 2000). The overall accuracy was calculated by dividing the number of pixels correctly classified (i.e. the sum of the diagonal axis) by the total number of pixels included in the evaluation process.

For individual classes, two accuracies were evaluated. The producer's accuracy is a measure of the omission error and indicates the percentage of pixels of a given vegetation type that is correctly classified. The user's accuracy is a measure of the commission error that indicates the probability that a pixel classified into a given class actually represents that class on the ground. Both the producer's and user's accuracies must be considered when analyzing the accuracy of a classification (Congalton 1991).

4.2.1 Maximum likelihood classification results

Maximum likelihood classification was performed. Table 3, 4 and 5 show the results from the ML classification for July, September and the combined images, respectively.

Table 3: Accuracy assessment of July image by ML classifier.

Class Name	Labels	Producer's Accuracy	User's Accuracy
Class 1	Water	98.00%	100.00%
Class 2	Forest	100.00%	97.78%
Class 3	Buildings	100.00%	89.23%
Class 4	Bare soil	88.10%	100.00%
Class 5	Agriculture area	53.25%	71.93%
Class 6	Grassland	81.19%	73.21%
Class 7	Herbaceous	90.48%	79.17%
Class 8	Swamp	88.46%	82.14%
Overall Accuracy	85.92%		

Table 4: Accuracy assessment of September image by ML classifier.

Class Name	Labels	Producer's Accuracy	User's Accuracy
Class 1	Water	100.00%	100.00%
Class 2	Forest	93.18%	78.85%
Class 3	Buildings	100.00	84.06%
Class 4	Bare soil	76.19%	94.12%
Class 5	Agriculture area	29.87%	76.67%
Class 6	Grassland	87.13%	67.18%
Class 7	Herbaceous	59.52%	64.10%
Class 8	Swamp	73.08%	54.29%
Overall Accuracy	78.78%		

Table 5: Accuracy Assessment of Combined Image by ML Classifier

Class Name	Labels	Producer's Accuracy	User's Accuracy
Class 1	Water	98.00%	100.00%
Class 2	Forest	100.00%	88.00%
Class 3	Buildings	100.00%	78.38%
Class 4	Bare soil	66.67%	100.00%
Class 5	Agriculture area	49.35%	59.38%
Class 6	Grassland	74.26%	72.12%
Class 7	Herbaceous	97.62%	80.39%
Class 8	Swamp	76.92%	95.24%
Overall Accuracy	82.04%		

When using only the July image, the overall classification accuracy was 85.92% (Table 3). The results for each class show moderate to high producer's and user's accuracies ranging from 53.25% to 100% and 71.93% to 100%, respectively. Water and bare soil have 100% user's accuracy, forest and buildings have 100% producer's accuracy. Agriculture area has the lowest producer's accuracy (53.25%) as well as users accuracy (71.93%) compared to other classes. This indicates that although 53.25% of the pixels were correctly classified as agriculture area, 71.93% of the areas labelled agriculture area actually belong to that class on the ground. Some substantial confusion is seen between, agriculture areas, grassland, herbaceous and swamp. Looking at Table 15 (Appendix III) we can see that mostly agriculture area and grassland have higher mixing than other classes which shows there is a spectral overlapping between these classes.

Using only the September image, the overall classification accuracy was 78.78% (Table 4). The results for each class show producer's and user's accuracies ranging from 29.87% to 100% and 54.29% to 100%, respectively. Water has both producer's and user's accuracy of 100% which is considered as a good sign of robustness (Congalton, 1991). This means that not only all pixels belonging to water were correctly classified as water but also 100% of the areas labelled water was actually water on the ground. Buildings

have 100% producer's accuracy. Similarly, as in the July image, the agriculture area has the lowest producer's accuracy (29.87%) but swamp has the lowest users accuracy (54.29%). Here also, the classes like 5, 6 and 7 are mixed with each other but significant mixing is seen between agriculture area and grassland. Mostly the agriculture areas are misclassified as grassland (Table 16, Appendix III). Table16 shows out of 77 pixels 38 are misclassified as grassland whereas only 23 are classified as agriculture area. This indicates that there's high spectral overlapping between these two classes. Some confusion is seen between buildings and bare soil. Few classes of swamp are also misclassified as forest.

When using the combined image, the overall classification accuracy was 82.04% (Table 5). The results show moderate to high producer's and user's accuracies ranging from 49.35% to 100% and 59.38% to 100%, respectively. The producer's and user's accuracies for most of the classes are better than in the September image but not as good as in the July image. Agriculture area still has the lowest producer's and user's accuracies (49.35%, 59.38%, respectively). There's still a substantial confusion seen between the classes 5, 6 and 7 (Table 17, Appendix III).

The overall accuracy is higher in the July image than in the September and combined images. The accuracies for almost all the classes are higher in the July image than in the September and combined images. We can also see in the spectral profiles of these images that the separation of various vegetation types is clearer in the July image than in others.

4.2.2 Minimum Distance classification results

Minimum Distance classification was also performed in order to compare the different classification methods. Table 6, 7 and 8 show the results from MD classifier for July, September and the combined images, respectively.

Table 6: Accuracy assessment of July image by MD Classifier

Class Name	Labels	Producer's Accuracy	User's Accuracy
Class 1	Water	100.00%	84.75%
Class 2	Forest	100.00%	84.62%
Class 3	Buildings	29.31%	65.38%
Class 4	Bare soil	73.81%	100.00%
Class 5	Agriculture area	79.22%	57.01%
Class 6	Grassland	64.36%	74.71%
Class 7	Herbaceous	40.4%	77.27%
Class 8	Swamp	30.7%	17.02%
Overall Accuracy	70.00%		

Table 7: Accuracy assessment of September image by MD classifier

Class Name	Labels	Producer's Accuracy	User's Accuracy
Class 1	Water	100.00%	75.19%
Class 2	Forest	90.91%	78.43%
Class 3	Buildings	41.38%	64.86%
Class 4	Bare soil	76.19%	100.00%
Class 5	Agriculture area	12.99%	71.43%
Class 6	Grassland	87.13%	73.95%
Class 7	Herbaceous	83.33%	50.72%
Class 8	Swamp	46.15%	34.29%
Overall Accuracy	69.59%		

Table 8: Accuracy assessment of Combined image by MD classifier

Class Name	Labels	Producer's Accuracy	User's Accuracy
Class 1	Water	100.00%	99.01%
Class 2	Forest	97.73%	89.58%
Class 3	Buildings	98.28%	83.82%
Class 4	Bare soil	73.81%	100.00%
Class 5	Agriculture area	68.83%	56.99%
Class 6	Grassland	58.42%	65.56%
Class 7	Herbaceous	35.71%	36.59%
Class 8	Swamp	65.38%	94.44%
Overall Accuracy	76.53%		

The result from the Minimum Distance classification shows that the overall classification accuracy for the July image was 70.00% (Table 6). The producer's and user's accuracies ranged from 29.31% to100.00% and from 17.02% to 100.00%, respectively. Water and forest have high (100%) producer's accuracy. Although bare soil has 73.81% of the pixels classified correctly as bare soil in the image, it has 100% user's accuracy, which means 100% of the areas labelled bare soil belong to that class on the ground. Swamp has both the producer's and user's accuracies lower than rest of the classes. Significant mixing is seen between classes 1, 3 and 8. Only 30.77% of the pixels are correctly classified as swamp and only 17.02% of the pixels are actually swamp on the ground. This is because most of the buildings are misclassified as swamp. Substantial mixing is seen within classes 5, 6, 7 and 8. Some confusion is seen within classes 2 and 8 too. Out of total 26 pixels, 8 are classified as swamp and 8 are misclassified as forest (Table 18, Appendix III).

The results from the September image show that the overall classification accuracy was 69.59% (Table 7). The results ranged from 12.99% to 100% producer's accuracy and from 34.29% to 100% user's accuracy. Although water has perfect producer's accuracy

(100%), the user's accuracy is only 75.19%. This means that all pixels belonging to water were correctly classified as water, but 75.19% of the areas labelled water were actually water on the ground. This is because most of the buildings are misclassified as water. Agriculture area has the lowest producer's accuracy (12.99%) but the user's accuracy is 71.43%. This indicates that, although only 12.99% of the agriculture area pixels were correctly classified as agriculture area, 71.43% of the areas labelled agriculture area actually belong to this class. Most agriculture areas are misclassified as grassland. Swamp also has quite low producer's and user's accuracies compared to other classes. High mixing is seen between class 1 and 3. Substantial mixing is seen within classes 5, 6, 7 and 8 (Table 19, Appendix III).

For the combined image (Table 8), it shows that the overall classification accuracy was 76.53%. The results for most of the classes show moderate to good producer's and user's accuracies ranging from 35.71% to 100% and 36.59% to 100%, respectively. The overall classification accuracy is higher than in the July and September image. Buildings and swamp have shown much improvement in the combined image than in the single image. Herbaceous has both producer's and user's accuracies lower than in the single image (35.71% and 36.59%, respectively). This is because most of the herbaceous are misclassified as grassland, 17 pixels out of 42 are misclassified as grassland and only 15 pixels are classified as herbaceous. Still, in the combined image, substantial mixing is seen within classes 5, 6 and 7 (Table 20, Appendix III). There is still spectral overlapping within these classes even in the combined image. From this we can depict that with the use of the MD classifier the accuracy is higher in the combined image than in the single image though there is still some confusion with some classes.

4.2.3 Decision Tree classification results

As mentioned in the methodology chapter, a different approach for vegetation classification i.e. Decision tree classification (CART analysis) was also used to see if there is any improvement in the classification results.

Decision tree classification proceeds by generating a tree (Figure 8). First of all, it generates it's own classification thresholds for each class deriving information from different bands. Then it recursively partitions the dataset into simpler forms.

The Figure 8, shows the decision tree obtained from CART. Each node contains a decision condition. All the leaf nodes represent class variables. Each class can have more than one leaf node. Every leaf node has a unique path from the root node, which forms a decision rule for that class.

For example, for Figure 9, (Appendix IV), a rule for Terminal Node 16, Class 2 (Forest) can be derived as

If B7 <= 131.3,

B10 > 80.5,

B1 > 79.5,

B4 > 109.5

Then Class = Class 2 (Forest)

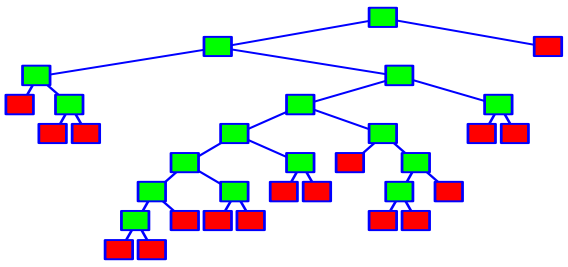

Figure 8: Example of decision tree generated by CART

One important aspect of this method is that after the classification, it ranks the importance of each band, which shows the contribution of each variable (band) in classifying or predicting the target variable, with the contribution coming from both the variable's role as a primary splitter and its role as a surrogate to any of the primary splitters. In the example (Table 9), band 4 is ranked as the most important one with 100% score, which contributed most to the classification process. Likewise, band 11 had the least contribution in the classification process with 29.79%.

Table 9: Variable Importance of each band

Variable	Score
B4	100.00
B1	97.42
B7	87.03
B5	85.81
B8	75.16
B2	57.96
B3	57.06
B10	53.56
B6	53.32
B9	42.70
B12	33.05
B11	29.79

The results from the DT classifier are shown in Table 10, 11 and 12 for July, September and combined images respectively.

Table 10: Accuracy assessment of July image by DT classifier.

Class Name	Labels	Producer's Accuracy	User's Accuracy
Class 1	Water	98.00%	100.00%
Class 2	Forest	97.72%	97.72%
Class 3	Buildings	86.20%	80.64%
Class 4	Bare soil	76.19%	96.96%
Class 5	Agriculture area	44.15%	75.55%
Class 6	Grassland	80.19%	70.43%
Class 7	Herbaceous	83.33%	58.33%
Class 8	Swamp	76.92%	60.60%
Overall Accuracy	80.20%		

Table 11: Accuracy assessment of September image by DT classifier.

Class Name	Labels	Producer's Accuracy	User's Accuracy
Class 1	Water	100.00%	97.08%
Class 2	Forest	90.90%	85.10%
Class 3	Buildings	93.10%	75.00%
Class 4	Bare soil	78.57%	86.84%
Class 5	Agriculture area	33.76%	72.22%
Class 6	Grassland	87.12%	72.72%
Class 7	Herbaceous	83.33%	53.03%
Class 8	Swamp	19.23%	71.42%
Overall Accuracy	77.75%		

Table 12: Accuracy assessment of combined image by DT classifier.

Class Name	Labels	Producer's Accuracy	User's Accuracy
Class 1	Water	99.00%	100.00%
Class 2	Forest	81.81%	90.00%
Class 3	Buildings	94.82%	84.61%
Class 4	Bare soil	83.33%	89.74%
Class 5	Agriculture area	48.05%	68.51%
Class 6	Grassland	65.34%	70.21%
Class 7	Herbaceous	90.47%	55.07%
Class 8	Swamp	57.69%	50.00%
Overall Accuracy	77.75%		

The results from the July image shows that the overall classification accuracy was 80.20% (Table 10). The results for different classes range from 44.15% to 98.00% producer's accuracy and from 58.33% to 100% user's accuracy. Class 2 shows good robustness in the accuracy as 97.72% of the pixels were correctly identified as forest and also 97.72% of the areas labeled forest were actually forest on the ground. Although agriculture area has quite high user's accuracy (75.55%), it has low producer's accuracy (44.15%), which is because most of the agriculture areas are misclassified as grassland. Some substantial confusion between classes 5, 6 and 7 is also seen with the DT classifier (Table 21, Appendix III).

The results from the September image shows that the overall classification accuracy is 77.75% (Table 11). The results show producer's accuracy ranging from 19.23% to 100% and user's accuracy ranging from 53.03% to 97.08%. Swamp has the lowest producer's accuracy (19.23%) but has quite high user's accuracy (71.42%), which shows 71.42% of the pixels belonging to the swamp class were actually swamp on the ground although

only 19.23% of the pixels were correctly classified. This is probably because most swamp classes are misclassified as forest, grassland and herbaceous. Here also, classes like 5, 6, 7 and 8 seem to mix with each other (Table 22, Appendix III).

The combined image also shows the same overall accuracy as in the September image of 77.75% (Table 12). The results for different classes show moderate to good producer's and user's accuracy ranging from 48.05% to 99% and 50% to 100%, respectively. Some classes like 3, 4, 5 and 7 have shown improved accuracy in comparison to the single image (Table 23, Appendix III).

4.3 Comparison between the three classifiers

The three classifiers ML, MD and DT were used for the classification of the vegetation along the floodplains.

Table 13: Classification accuracy comparisons between different classifiers.

	Overall Classification Accuracy		
	ML classifier	MD classifier	DT classifier
July image	85.92%	70.00%	80.20%
September image	78.78%	69.59%	77.75%
Combined image	82.04%	76.53%	77.75%

From Table 13, we can see that the overall classification accuracy for ML, MD and DT classifiers are almost similar. The ML classifier seems to have higher accuracy than the other classifiers. The accuracy for the July image is higher than for the September image with all the three classifiers. This may be because the July image was very clear whereas the September image had some cloud cover. Also in the July image the spectral reflectance of various vegetation types are more separable than in the September image (Figures 5 and 6). This may be perhaps because in July the vegetation has peak greenness, which are more easily separated. More confusion seen between agriculture area and grassland can be because some agriculture areas may have been already harvested at the time the September image was acquired, being left bare or with some grasses. This shows that seasonality plays an important role in classification of vegetation (Schriever & Congalton, 1995). The best season for vegetation classification could be July when there is peak greenness.

5 Conclusion and Recommendations

The main objective of the study was to compare the different types of classification methods used in remote sensing for a multitemporal analysis for classifying vegetation in the floodplain along the river Waal. For this purpose three different classifiers ML, MD and DT were successfully applied for single as well as the combined images.

This study provided some analysis of the use of different classification methods used in remote sensing and also the use of combined image for vegetation classification along the floodplains. Images of two dates were also successfully merged for use in multitemporal analysis.

The results obtained from the three classifiers were quite satisfactory. Comparatively, the classification with combined imagery showed satisfactory result with the MD classifier compared to ML and DT classifiers. Classes 1, 2, 3 and 4 were quite well classified by all the classifiers in all the images. Classes 5, 6, 7 and 8 seem to be overlapping with each other in all the images. Basically, none of the approaches could well discriminate the classes from 5 to 8. This concludes that these classes have similar spectral reflectances so they couldn't be classified well. For most of the classes, the producer's and the user's accuracies were higher in the July image than in the others. A July image allowed for better discrimination of the various vegetation types.

Among the three classifiers, the ML classifier was found to be better than the MD and DT classifiers. All the classifiers reveal the similar kind of results regarding the mixing problem of classes 5, 6, 7 and 8. But an advantage of the DT classifier over the others was that it created variable importance for each band, which was useful to understand the contribution of each band for the classification.

Above all, what can be concluded is that the multitemporal analysis is quite useful to classify the images of different times and see the changes, though the accuracy largely depends on the quality of the data, the methods used and on the reference data.

The recommendations concerning further studies can be summarized as

- Getting a prior knowledge about the study area before performing any classification is very vital in remote sensing. Only using the images and the aerial pictures cannot get high accuracy results. It is advisable to make use of other ancillary data as well.
- The success of a classification depends not only on the land cover and remotely sensed data type, but also on the classification method (Kenk et al., 1988), season (Wolter et al., 1995, Schriever and Congalton, 1995), and to a large extend on reference data (Congalton, 1991). So, it is recommended to have proper ground truth data collected by GPS, which is very necessary to be used for the accuracy assessment.
- Decision tree classifiers have shown to be influenced by the number of training samples used for the various classes (Friedl & Brodley, 1997), with smaller classes often being penalized over classes with more numerous training samples. So, it could be better if a larger number of training samples are used for the decision tree classifier to get more accurate results.
- Looking at the results, classes like 5, 6 and 7 could be merged to one class and class 2 and 8 could also be merged since they show significant overlapping with each other. These classes then could be well separated with the available dataset.
- As far as the multitemporal analysis is concerned, a better approach for combining the images of different times could be found so that the changes could be seen more easily.

References

Asselman., N.E.M. (2001). Sediment processes in the floodplains. Delft Cluster & IRMA-SPONGE programme, CFR project report 8. WL/Delft Hydraulics

Badhwar, G. D., Carnes, J. G., & Austin, W. W. (1982). Use of Landsat-derived temporal profiles for corn-soyabean feature extraction and classification. Remote sensing of Environment. 12:57-79.

Breiman, L., Friedman, J. H., Olshen, R. A., & Stone, C. J. (1984). Classification and Regression Trees. Wadsworth, Belmont, CA.

Brodley, C. E., & Utgoff, P. E. (1995). Multivariate decision trees, Mach. Learn. 19:45-77.

Brown de Colstoun, E. C., Story, M. H., Thompson, C., Commisso, K., Smith, T. G., & Irons, J. R. (2003). National Park vegetation mapping using multitemporal Landsat 7 data and a decision tree classifier. Remote Sensing of Environment, 85, 316- 327.

Campbell, J. B. (1996). Introduction to remote Sensing. Second Edition, Taylor & Francis.

Congalton, R. G. (1991). A review of assessing the accuracy of classifications of remotely sensed data. Remote Sensing of Environment, 37, 35-46.

Cracknell, A. P., 1999. Twenty years of publication of the International Journal of Remote Sensing. International Journal of Remote Sensing, 20, 3469-3484.

Dai, X., & Khorram, S. (1998). Hierarchical methodology framework for multisource data fusion in vegetation classification. International Journal of Remote Sensing, 19, 3697-3701.

DeFries, R. S., & Townshend, J. R. G. (1994). NDVI-derived land cover classification at global scales. International Journal of Remote Sensing. 15: 3567-3586.

Friedl, M. A., & Brodley, C. (1997). Decision tree classification of land cover from remotely sensed data. Remote Sensing of Environment, 61, 399- 409.

Friedl, M. A., Brodley, C. E., & Strahler, A. (1999). Maximizing land cover classification accuracies produced by decision trees at continental to global scales. IEEE Trans. Geosci. Remote Sens. 37:969-977.

Geerling, G. W., Peters, B., & Smits, A. J. M. (2001). Development of floodplain ecotopes in the Netherlands (Rhine tributaries). CFR project report 6. University of Nijmegen.

Hansen, M., DeFries, R., Townshend, J. R. G., & Sohlberg, R. (2000). Global land cover classification at 1 km spatial resolution using a classification tree approach. International Journal of Remote Sensing. 21:1331-1364.

Hansen, M., Dubayah, R., & DeFries, R. (1996). Classification trees: an alternative to traditional land cover classifiers. International Journal of Remote Sensing , 17, 1075-1081.

IKSR, 1997. Hochwasserschutz am Rhein. Bestandsaufname. Koblenz.

Jeon, B., & Landgrebe, D. A. (1999). Decision fusion approach for multitemporal classification. IEEE Transactions on Geoscience and Remote Sensing, 37, 1227-1233.

Kalensky, Z., & Scherk, R. R. (1975). Accuracy of forest mapping from Landsat computer compatible tapes. Proc. 10th Int. Symp. Remote Sens. Environ., 6-10 October, Ann Arbor.

Kenk, E., Sondheim, M., & Yee, B. (1988). Methods for improving accuracy of Thematic Mapper ground cover classification. Canadian Journal of Remote Sensing, 17, 1075-1081.

Landsat 5, Sensor characteristics, 2004.

http://www.spaceimagingme.com/content/Constellation/Landsat/index.asp

Lawrence, R. L., & Wright, A. (2001). Rule-Based Classification systems using classification and regression tree (CART) analysis. Photogrammetric Engineering & Remote Sensing, 67, 1137-1142.

Leopold, LB., Wolman, M. G., & Miller, J. P. Fluvial Processes in Geomorphology (San Francisco, California: W.H. Freeman, 1964).

Lewis, R. J., (2000). An Introduction to Classification and Regression Tree (CART) Analysis. Department of Emergency Medicine, Harbor-UCLA Medical Center, Torrance, California.

Lillisand, T. M., & Kiefer, R. W. (2000). Remote Sensing and Image Interpretation.

Loveland, T. R., & Belward, A. S. (1997). The IGBP-DIS global 1 km land cover data set, DISCover: first results. International Journal of Remote Sensing. 18:3289-3295.

Liu, Q. J., Takamura, T., Takeuchi, N., & Shao, G. (2002). Mapping of boreal vegetation of a temperate mountain in China by multitemporal Landsat TM imagery. International Journal of Remote Sensing, VOL. 23, NO. 17, 3385- 3405

Michelson, D. B., Liljeberg, B. M., & Pilesjo, P. (2000). Comparison of algorithms for classifying Swedish landcover using Landsat TM and ERS-1 SAR data. Remote Sensing of Environment, 71(1), 1-15.

Pavuluri, M. K. (2003). Fuzzy Decision Tree Classification for High-Resolution Satellite Imgaery. University of Missouri-Columbia.

Pax-Lenney, M., & Woodcock, C. E. (1997). Monitoring Agricultural lands in Egypt with Multitemporal Landsat TM Imagery: How Many Images Are Needed?. Remote Sensing of Environment, 59, 522- 529.

Quinlan, J. R. (1993). C4.5: programs for machine learning. San Mateo, CA: Morgan Kaufman Publishers.

Salford Systems White Paper Series. http://www.salford-systems.com/whitepaper.html

Safavian, S. R., & Landgrebe, D. (1991). A survey of decision tree classifier methodology. IEEE Transactions on Systems, Man, and Cybernetics, 21, 660-674.

Schmudde, T.H. "Floodplain"in R.w. Fairbridge, The Encyclopedia of Geomorphology (New York: Reinhold, 1968).

Schriever, J. R., & Congalton, R. G. (1995). Evaluating seasonal variability as an aid to cover-type mapping from Landsat Thematic Mapper data in the northeast. Photogrammetric Engineering & Remote Sensing, 61, 321-327.

Song, C., & Woodcock, C. E. (2003). Monitoring Forest Succession With Multitemporal Landsat Images: Factors of Uncertainty. IEEE Transactions on Geoscience and Remote Sensing, Vol. 41, No. 11, November 2003.

Steiner, D., & Maurer, H. (1969). The use of stereo height as a discriminating variable for crop classification on aerial photographs. Photogrammetria 24:223-241.

Swain, P. H., & Hauska, H. (1977). The decision tree classifier: design and potential. IEEE Trans. Geosci. Electron. GE-15:142-147.

Swain, P. H., & Hauska, H. (1969). The decision tree classifier: design and potential. IEEE Trans. Geosci. Remote sens. GE-15:142-147.

Tucker, C. J., Townshend, J. R. G., & Goff, T. E. (1985). African land-cover classification using satellite data. Science 227:369-375.

Van der Lee, G. E. M., Baptist, M.J., Ververs, M., & Geerling, G. W. (2001). Application of the Cyclic Floodplain Rejuvenation strategy to the Waal river. CFR project report 15. WL / Delft Hydraulics, Delft University of Technology, University of Nijmegen.

Vogelmann, J. E. et al. (2001). Completion of the 1990s national land cover data set for the conterminous United States from Landsat Thematic Mapper and ancillary data sources. Photogrammetric Engineering & Remote Sensing, 67, 650-662.

Wagner, D. G., Hoffer, R. M., & Hanson, J. D. (1993). Comparison of multitemporal and unitemporal classification accuracy using Landsat TM imagery. In Looking to the Future with an Eye on the Past (A. J. Lewis, Ed.), ACSM/ASPRS Convention, New Orleans, LA.

Wolter, P.T., Mladenoff, D. J., Host, G. E., & Crow, T. R. (1995). Improved forest classification in the northern lake states using multitemporal Landsat imagery. Photogramm. Eng. Remote Sens. 61(9): 1129-1143.

Appendices

Appendix I: Dataset Projection Information

Projection Type	Stereographic
Spheroid Name	Bessel
Datum Name	Bessel
Longitude of center of projection	5:23:15.500000E
Latitude of center of projection	52:09:22.178000N
False easting	155000.000000meters
False northing	463000.000000meters

Appendix II: Ecotope Translation

Table 14: Ecotope Translation

Code	Ecoid (English)	Omschrijvi (Dutch)
RWp-1	water	Aangekoppeld zand/grindgat
RWs-1	water	Aangekoppelde strang
RWp-2	water	Afgesloten zand/grindgat
RWs-2	water	Afgesloten/stagnante strang
RHr-3	buildings	Bebouwd hoogwatervrij terrein
ROr-4	buildings	Bebouwde oeverwal
RUr-4	buildings	Bebouwde uiterwaard
RWs-5	water	Beekstrang
RZd-1	water	Diepe bedding
RWn-3	water	Getijdekreek
RWp-4	water	Haven
RHb-2	forest	Hoogwatervrij (doorn)struweel
RHb-2	forest	Hoogwatervrij (zachthout)struweel
RHb-1	forest	Hoogwatervrij bos (hardhout)
RHb-1	forest	Hoogwatervrij bos (zachthout)
RHb-3	forest	Hoogwatervrij produktiebos (hardhout)
RHb-3	forest	Hoogwatervrij produktiebos (zachthout)
RHg-3	grassland	Hoogwatervrij produktiegrasland
RHg-1	grassland	Hoogwatervrij schraalgrasland
RHr-2	agriculture area	Hoogwatervrije akker
RWp-3	water	Klein diep water/kolk
RMr-1	swamp	Moerasruigte
RMb-4	forest	Moerassig broekbos/struweel
RMb-1	forest	Moerassig hardhoutooibos
RMg-2	grassland	Moerassig produktiegrasland
RMg-1	grassland	Moerassig uiterwaardgrasland
RMb-2	forest	Moerassig zachthoutooibos
RMb-3	forest	Moerassig zachthoutstruweel
ROr-3	agriculture area	Oeverwal akker
ROb-2	forest	Oeverwal doornstruweel
ROb-1	forest	Oeverwal hardhoutooibos
ROr-1	bare soil	Oeverwal met rivierduinvorming

ROb-5	forest	Oeverwal produktiebos (hardhout)
ROb-5	forest	Oeverwal produktiebos (zachthout)/griend
ROg-3	grassland	Oeverwal produktiegrasland
ROg-1	grassland	Oeverwal stroomdalgrasland
ROb-3	forest	Oeverwal zachthoutooibos
ROb-4	forest	Oeverwal zachthoutstruweel
RHk-1	bare soil	Onbegroeid hoogwatervrij terrein
ROk-1	bare soil	Onbegroeide oeverwal
RUk-1	bare soil	Onbegroeide uiterwaard
RZo-2	bare soil	Ondiepe zandbedding
RMr-2	swamp	Rietmoeras
RZs-3	swamp	Slikplaten/slikkige oever
ROr-2	herbaceous	Soortenarme oeverwalruigte
RHr-1	herbaceous	Soortenarme ruigte op hoogwatervrij terrein
RUr-2	herbaceous	Soortenarme uiterwaardruigte
RUg-1	grassland	Structuurrijk uiterwaardgrasland
ROr-2	herbaceous	Structuurrijke oeverwalruigte
RHr-1	herbaceous	Structuurrijke ruigte op hoogwatervrij terrein
RUr-1	herbaceous	Structuurrijke uiterwaardruigte
RUr-3	agriculture area	Uiterwaard akker
RUb-2	forest	Uiterwaard doornstruweel
RUb-5	forest	Uiterwaard hardhout produktiebos
RUb-1	forest	Uiterwaard hardhoutooibos
RUg-3	grassland	Uiterwaard produktiegrasland
RUb-6	forest	Uiterwaard zachthout produktiebos/griend
RUb-3	forest	Uiterwaard zachthoutooibos
RUb-4	forest	Uiterwaard zachthoutstruweel
RHr-3	buildings	Verhard hoogwatervrij terrein
ROr-4	buildings	Verharde oeverwal
RUr-4	buildings	Verharde uiterwaard
RWn-1	water	Zandige nevengeul
RZs-2	bare soil	Zandplaat/zandstrand

Dutch variables for the species algorithms in `A stream Nature`	English translation	Equivalence between variables of `A stream Nature` species algorithms and official ecotope types as defined in the RES (River Ecotope System)	Caption	Our ecotope classification	Caption
ZD	RD	Zd	deep riverbed	RD	Deep Riverbed
ZO	RS	Zo	shallow riverbed	RS	Shallow Riverbed
ON	B	Zs1, Zs2, Zs3, Zs4, Zs5	Bar, beach, natural bank	B B_s	flat river Bank Steep Bank / eroding bank (Zs5for the river, or else)
BZ BM	FS FM	Ob3, Ob4, Ub3, Ub4, Mb2, Mb3 Mb4	softwood floodplain forest or dominated by willows marsh forest	FSM	floodplain Forest with Softwood and Marsh forest
BH	FH	Ob1, Ob2, Ub1, Ub2, Mb1, Hb1, Hb2	ecotope hardwood floodplain forest	FH	floodplain Forest with Hardwood
M	M	Mr2, Mr3	marsh	M	Marsh (plus Mr1 and minus Mr2)
	P	Mr2	reed	P_y P_o	Young Phragmites reed (harvested every year) Old Phragmites reed (not harvested every year)
GO GU RU	GO GF UF	Og1, Hg1 Og2, Ug1, Ug2, Mg1, Mg3, Hg2 Ur1, Ur2, Mr1	pasture floodplain grassland floodplain underwood (minus Mr1)	GP	Grassland Pasture (minus Mr1)
RO	HD	Or1, Or2, Hr1	herbaceous natural levee and river dunes	HD	Herbaceous natural levee and river Dunes (plus Ok-1, added to RES)
GP	AG	Og3, Ug3, Mg2, Hg3	production grassland	GM	Grassland Meadow
WN	WS	Wn1, Wn2, Wn3	secondary channel / side channel	WS	Water formed by a Secondary channel
WD	WD	Ws1, Ws2, Ws4, Ws5	water dynamic blind river arm	WD	Dynamic blind river arm Water)
WS	WI	Ws3, Wp3	isolated blind river arm	WI	Isolated blind river arm Water
WP	WP	Wp1, Wp2	pool	WP	Pool Water
S OS	MB MR	Or4, Ur4, Hr3 Zs6	manmade buildings manmade rocky bank	MB	Manmade Buildings (sensu lato)
				MW	Manmade water (harbour, intensive recreation…) (Wp4, added to RES)
LA BP	AA AF	Or3, Ur3, Hr2 Ob5, Ub5, Ub6, Hb3	arable land (crop land) production forest	A	Agricultural land (production forest, crop land)
	H		hedges	H	Hedges
	D		ditches	D	Ditches

Assumptions

- The area of the water bodies on the map correspond with the area of the water bodies checked in the field June 1998.

Remarks

- The ecotope concept is not relevant for the description of species habitats. For instance, it is very often important to distinguish whether an ecotope (especially aquatic ecotope) is covered with vegetation or not.
- Some ecotope types were added to the original 1994 Rademakers *et al*. RES (Ok1, Wp4…)

The ecotope types used for habitat suitability must be an exact combination of MORRES ecotope types (Duel *et al.*, 1996), in order to allow comparison of MORRES and OUR models. Only ecotopes types not relevant for target species can be grouped in quite a free way (e.g. : grassland)

Appendix III: Accuracy assessment results

Table 15: Error Matrix, Maximum likelihood classification (July Image)

Reference data										
Classes	Class 1	Class 2	Class 3	Class 4	Class 5	Class 6	Class 7	Class 8	Row Total	User's Accuracy
Class 1	**98**	0	0	0	0	0	0	0	98	**100%**
Class 2	0	**44**	0	0	0	0	0	1	48	**97.78%**
Class 3	2	0	**58**	5	0	0	0	0	65	**89.23%**
Class 4	0	0	0	**37**	0	0	0	0	37	**100.00%**
Class 5	0	0	0	0	**41**	16	0	0	57	**71.93%**
Class 6	0	0	0	0	27	**82**	2	1	112	**73.21%**
Class 7	0	0	0	0	9	0	**38**	1	48	**79.17%**
Class 8	0	0	0	0	0	3	2	**23**	28	**82.14%**
Column Total	100	44	58	42	77	101	42	26	**490**	
Producer's accuracy	**98%**	**100%**	**100%**	**88.10%**	**53.25%**	**81.19%**	**90.48%**	**88.46%**		
Overall Classification accuracy = 85.92%						Kappa Statistics = 0.8347				

Table 16: Error Matrix, Maximum likelihood classification (September Image)

Reference Data										
Classes	Class 1	Class 2	Class 3	Class 4	Class 5	Class 6	Class 7	Class 8	Row Total	User's accuracy
Class 1	**100**	0	0	0	0	0	0	0	100	**100%**
Class 2	0	**41**	0	0	1	0	4	6	52	**78.85%**
Class 3	0	0	**58**	10	0	0	1	0	69	**84.06%**
Class 4	0	0	0	**32**	0	0	2	0	34	**94.12%**
Class 5	0	2	0	0	**23**	4	1	0	30	**76.67%**
Class 6	0	0	0	0	38	**88**	4	1	131	**67.18%**
Class 7	0	0	0	0	5	9	**25**	0	39	**64.10%**
Class 8	0	1	0	0	10	0	5	**19**	35	**54.29%**
Column Total	100	44	58	42	77	101	42	26	**490**	
Producer's accuracy	**100%**	**93.18%**	**100%**	**76.19%**	**29.87%**	**87.13%**	**59.52%**	**73.08%**		
Overall Classification accuracy = 78.78%						Kappa Statistics = 0.7506				

Table 17: Error Matrix, Maximum likelihood classification (Combined Image)

Reference Data										
Classes	Class 1	Class 2	Class 3	Class 4	Class 5	Class 6	Class 7	Class 8	Row Total	User's accuracy
Class 1	**98**	0	0	0	0	0	0	0	98	**100%**
Class 2	0	**44**	0	0	0	0	0	6	50	**88%**
Class 3	2	0	**58**	14	0	0	0	0	74	**78.38%**
Class 4	0	0	0	**28**	0	0	0	0	28	**100%**
Class 5	0	0	0	0	**38**	26	0	0	64	**59.38%**
Class 6	0	0	0	0	29	**75**	0	0	104	**72.12%**
Class 7	0	0	0	0	10	0	**41**	0	51	**80.39%**
Class 8	0	0	0	0	0	0	1	**20**	21	**95.24%**
Column Total	100	44	58	42	77	101	42	26	**490**	
Producer's accuracy	**98%**	**100%**	**100%**	**66.67%**	**49.35%**	**74.26%**	**97.62%**	**76.92%**		
Overall Classification accuracy = 82.04%						Kappa Statistics = 0.7892				

Table 18: Error Matrix, Minimum Distance classification (July Image)

Reference Data										
Classes	Class 1	Class 2	Class 3	Class 4	Class 5	Class 6	Class 7	Class 8	Row Total	User's accuracy
Class 1	**100**	0	13	2	0	0	0	3	118	**84.75%**
Class 2	0	**44**	0	0	0	0	0	8	52	**84.62%**
Class 3	0	0	**17**	9	0	0	0	0	26	**65.38%**
Class 4	0	0	0	**31**	0	0	0	0	31	**100%**
Class 5	0	0	0	0	**61**	35	9	2	107	**57.01%**
Class 6	0	0	0	0	16	**65**	5	1	87	**74.71%**
Class 7	0	0	0	0	0	1	**17**	4	22	**77.27%**
Class 8	0	0	28	0	0	0	11	**8**	47	**17.02%**
Column Total	100	44	58	42	77	101	42	26	**490**	
Producer's accuracy	**100%**	**100%**	**29.31%**	**73.81%**	**79.22%**	**64.36%**	**40.48%**	**30.77%**		
Overall Classification accuracy = 70.00%						Kappa Statistics = 0.6470				

Table 19: Error Matrix, Minimum Distance classification (September Image)

Reference Data										
Classes	Class 1	Class 2	Class 3	Class 4	Class 5	Class 6	Class 7	Class 8	Row Total	User's accuracy
Class 1	**100**	0	30	1	0	0	0	2	133	**75.19%**
Class 2	0	**40**	4	0	0	0	2	5	51	**78.43%**
Class 3	0	0	**24**	8	3	0	2	0	37	**64.86%**
Class 4	0	0	0	**32**	0	0	0	0	32	**100%**
Class 5	0	0	0	0	**10**	4	0	0	14	**71.43%**
Class 6	0	0	0	1	26	**88**	3	1	119	**73.95%**
Class 7	0	1	0	0	18	9	**35**	6	69	**50.72%**
Class 8	0	3	0	0	20	0	0	**12**	35	**34.29%**
Column Total	100	44	58	42	77	101	42	26	**490**	
Producer's accuracy	**100%**	**90.91%**	**41.38%**	**76.19%**	**12.99%**	**87.13%**	**83.33%**	**46.15%**		
Overall Classification accuracy = 69.59%						Kappa Statistics = 0.6424				

Table 20: Error Matrix, Minimum Distance classification (Combined Image)

Reference Data										
Classes	Class 1	Class 2	Class 3	Class 4	Class 5	Class 6	Class 7	Class 8	Row Total	User's accuracy
Class 1	**100**	0	1	0	0	0	0	0	101	**99.01%**
Class 2	0	**43**	0	0	0	0	0	5	48	**89.58%**
Class 3	0	0	**57**	11	0	0	0	0	68	**83.82%**
Class 4	0	0	0	**31**	0	0	0	0	31	**100%**
Class 5	0	1	0	0	**53**	27	9	3	93	**56.99%**
Class 6	0	0	0	0	13	**59**	17	1	90	**65.56%**
Class 7	0	0	0	0	11	15	**15**	0	41	**36.59%**
Class 8	0	0	0	0	0	0	1	**17**	18	**94.44%**
Column Total	100	44	58	42	77	101	42	26	490	
Producer's accuracy	**100%**	**97.73%**	**98.28%**	**73.81%**	**68.83%**	**58.42%**	**35.71%**	**65.38%**		
Overall Classification accuracy = 76.53%						Kappa Statistics = 0.7240				

Table 21: Error Matrix, Decision Tree classification (July Image)

Reference Data										
Classes	Class 1	Class 2	Class 3	Class 4	Class 5	Class 6	Class 7	Class 8	Row Total	User's accuracy
Class 1	**98**	0	0	0	0	0	0	0	98	**100%**
Class 2	0	**43**	0	0	0	0	1	0	44	**97.72%**
Class 3	2	0	**50**	10	0	0	0	0	62	**80.64%**
Class 4	0	0	0	**32**	0	0	1	0	33	**96.96%**
Class 5	0	1	0	0	**34**	7	0	3	45	**75.55%**
Class 6	0	0	0	0	33	**81**	1	0	115	**70.43%**
Class 7	0	0	0	0	10	12	**35**	3	60	**58.33%**
Class 8	0	0	8	0	0	1	4	**20**	33	**60.60%**
Column Total	100	44	58	42	77	101	42	26	**490**	
Producer's accuracy	**98%**	**97.72%**	**86.20%**	**76.19%**	**44.15%**	**80.19%**	**83.33%**	**76.92%**		
Overall Classification accuracy = 80.20%										

Table 22: Error Matrix, Decision Tree classification (September Image)

Reference Data										
Classes	Class 1	Class 2	Class 3	Class 4	Class 5	Class 6	Class 7	Class 8	Row Total	User's accuracy
Class 1	**100**	1	1	0	0	0	0	1	103	**97.08%**
Class 2	0	**40**	2	0	0	0	0	5	47	**85.10%**
Class 3	0	0	**54**	9	5	0	4	0	72	**75.00%**
Class 4	0	0	0	**33**	4	1	0	0	38	**86.84%**
Class 5	0	1	0	0	**26**	3	0	6	36	**72.22%**
Class 6	0	0	0	0	29	**88**	2	2	121	**72.72%**
Class 7	0	2	1	0	12	9	**35**	7	66	**53.03%**
Class 8	0	0	0	0	1	0	1	**5**	7	**71.42%**
Column Total	100	44	58	42	77	101	42	26	**490**	
Producer's accuracy	**100%**	**90.90%**	**93.10%**	**78.57%**	**33.76%**	**87.12%**	**83.33%**	**19.23%**		
Overall Classification accuracy = 77.75%										

Table 23: Error Matrix, Decision Tree classification (Combined Image)

Reference Data										
Classes	Class 1	Class 2	Class 3	Class 4	Class 5	Class 6	Class 7	Class 8	Row Total	User's accuracy
Class 1	**99**	0	0	0	0	0	0	0	99	**100.00%**
Class 2	0	**36**	0	0	0	0	0	4	40	**90.00%**
Class 3	1	0	**55**	7	0	0	0	2	65	**84.61%**
Class 4	0	0	1	**35**	0	3	0	0	39	**89.74%**
Class 5	0	2	0	0	**7**	14	0	1	54	**68.51%**
Class 6	0	0	0	0	35	**66**	3	0	94	**70.21%**
Class 7	0	3	0	0	0	18	**38**	4	69	**55.07%**
Class 8	0	3	2	0	0	0	1	**15**	30	**50.00%**
Column Total	100	44	58	42	77	101	42	26	**490**	
Producer's accuracy	**99%**	**81.81%**	**94.82%**	**83.33%**	**48.05%**	**65.34%**	**90.47%**	**57.69%**		
Overall Classification accuracy = 77.75%										

Appendix IV: Decision tree generated by CART

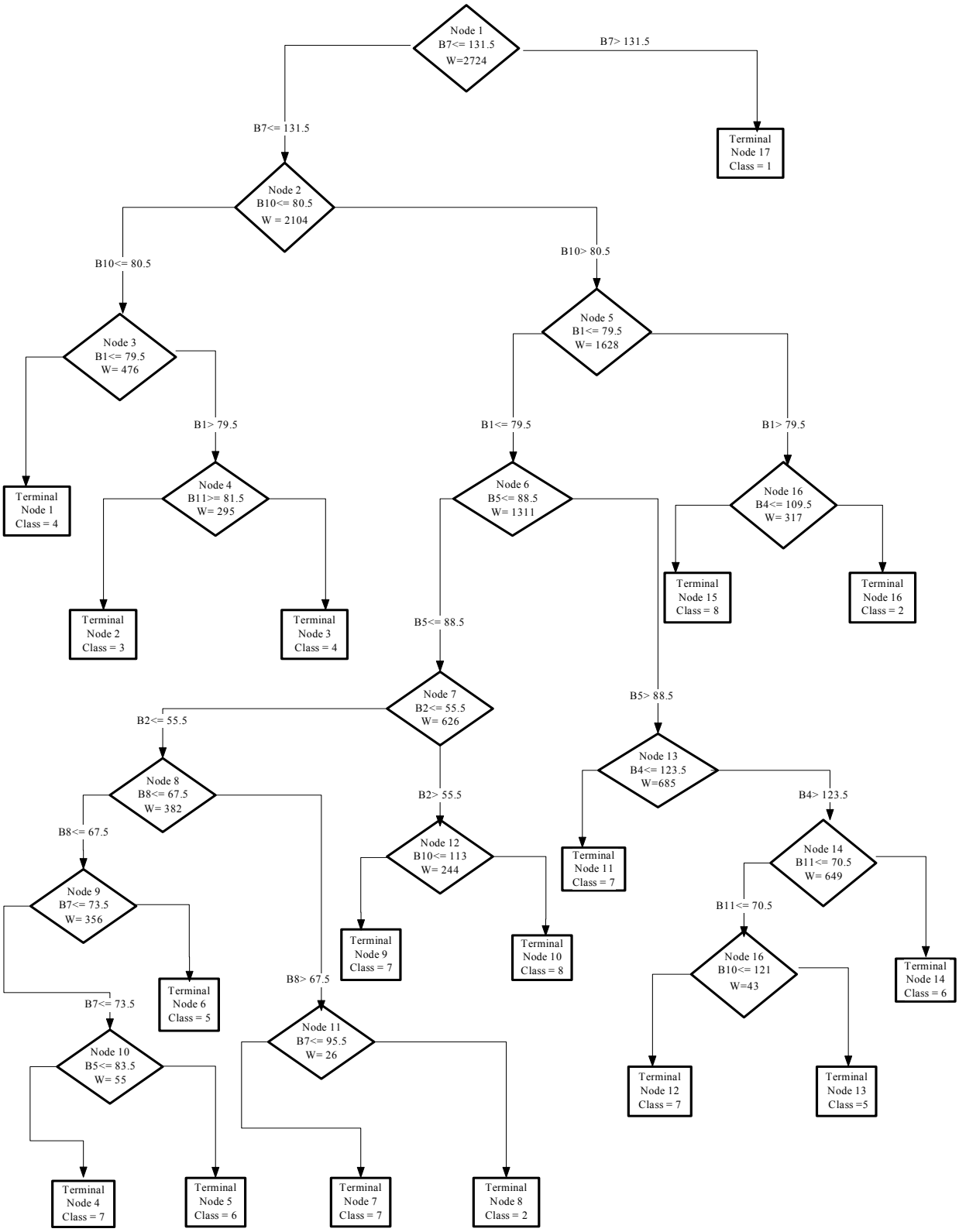

Figure 9: Decision tree generated by CART